geoconvention
Calgary • Canada • May 11-13 2026

Combining active and passive seismic sensing for CO_2 monitoring

Xiaohui Cai[1], Kristopher Innanen[1], Tianze Zhang[1]

[1] Department of Earth, Energy, and Environment, CREWES Project, University of Calgary

Summary

Effective monitoring of subsurface CO_2 migration requires seismic methods that combine high spatial resolution with dense temporal sampling. Active-source time-lapse full-waveform inversion (FWI) can image CO_2-induced velocity changes with high fidelity; however, repeat surveys are typically conducted at sparse time intervals due to operational and economic constraints, leaving critical phases of plume evolution poorly constrained. Injection-induced microseismicity, which can be continuously recorded by downhole distributed acoustic sensing (DAS) arrays, provides a quasi-continuous passive wavefield capable of bridging these temporal gaps. In practice, however, passive-source FWI is strongly limited by source uncertainty, which often leads to unstable inversions and cycle skipping. We propose a joint active–passive time-lapse FWI framework for quasi-continuous CO_2 monitoring that integrates sparse active surveys with dense passive microseismic observations. Active-source FWI is used to establish reliable baseline and final monitor models, while passive microseismic data provide intermediate time-lapse updates. To mitigate the impact of source uncertainty, we develop a robust source-independent FWI strategy that significantly reduces sensitivity to wavelet mismatch. Numerical experiments across six CO_2 injection stages demonstrate that the proposed approach stably recovers the primary CO_2-related velocity anomalies and their migration trends, even under strong source mismatch. The results indicate that microseismic wavefields, when incorporated through source-tolerant formulations, can effectively complement active surveys and provide a practical pathway toward quasi-continuous seismic monitoring of geological CO_2 storage.

Method

FWI has become an established tool for recovering detailed subsurface models (Virieux and Operto, 2009; Prieux et al., 2013; Pan et al., 2020; Huang et al., 2021; Vigh et al., 2023; Hu et al., 2023). When applied to vertical seismic profile (VSP) data, FWI benefits from strong well-log constraints that reduce parameter non-uniqueness (O'Brien et al., 2004; Asnaashari et al., 2013; Aragao and Sava, 2020; Cai et al., 2024; Hu et al., 2024; Zhang et al., 2025). Active-source time-lapse FWI has demonstrated the ability to image CO_2-induced velocity changes with high spatial resolution (Egorov et al., 2017; Isaenkov et al., 2022); however, repeat surveys are typically separated by months to years. As a result, important phases of plume evolution—such as early breakthrough and subsequent migration—remain undersampled. Recent advances in rapid-repeat active-source monitoring have shown that denser temporal sampling can capture short-term CO_2 plume dynamics (Cai et al., 2025). Nevertheless, maintaining continuous repeat acquisition requires activating controlled sources at rates that are operationally and economically difficult to sustain. This limitation motivates the need for an alternative source of quasi-continuous seismic information that can complement, rather than replace, repeat active surveys.

To address this challenge, we adopt a joint active–passive time-lapse FWI framework. Active-source FWI is first performed on baseline data to construct a reliable background velocity model. During CO_2 injection, microseismic events—quasi-continuously recorded by downhole DAS

arrays—provide time-dense passive wavefields that supplement the active-source constraints. Finally, active-source FWI of the monitor data is used to resolve the cumulative CO_2 plume anomaly. This joint strategy exploits the complementary strengths of the two data types: active-source FWI provides high-resolution and stable model updates, while passive microseismic observations enable dense temporal sampling without additional acquisition cost.

For the active-source component, we employ an L1 waveform-difference misfit, which is more robust to noise and less sensitive to amplitude and arrival-time mismatches, thereby reducing the risk of cycle skipping. In contrast, passive-source FWI differs fundamentally from active-source inversion in that the source properties are not controlled. For microseismic events, the source wavelet, origin time, and sometimes even the source location are only approximately known. Uncertainty in these parameters introduces phase and amplitude inconsistencies between observed and modeled data, which can severely degrade conventional waveform-based inversion. To mitigate source uncertainty in passive microseismic FWI, three source-independent or source-tolerant inversion strategies are considered and compared in this study. The first approach employs an envelope-based misfit, which replaces waveform amplitudes with their envelopes. By suppressing phase sensitivity, this formulation reduces the impact of wavelet and origin-time mismatch and primarily recovers low-wavenumber velocity updates, improving stability at the expense of spatial resolution. The second approach adopts Choi's source-independent objectives that eliminate explicit dependence on the source wavelet. This strategy further weakens source-related effects and enhances kinematic consistency compared with envelope-only objectives, while remaining independent of an accurate source estimate. The third approach is the proposed method, which is also source-independent but is formulated using a symmetric cross-correlation structure that explicitly exchanges the role of the source wavelet between modeled and observed data. Rather than removing the source term implicitly, the method introduces a weighted convolution in which the estimated wavelet from one dataset is applied to the other, and vice versa. This exchange mechanism balances source effects between the two wavefields and suppresses source-induced asymmetry in the misfit.

Results

We first present results from conventional repeat active-source VSP FWI to establish a reference for time-lapse CO_2 monitoring. Using a fixed and known source wavelet (Figure 1), the baseline and final monitor inversions accurately recover the large-scale velocity structure as well as the CO_2-induced ΔV_p anomaly. The inverted time-lapse model (Figure 2) closely matches the true plume geometry, and the misfit curve (Figure 3) decreases smoothly and stabilizes, indicating a well-conditioned inversion.We next examine passive microseismic FWI under idealized conditions in which the passive-source wavelet is assumed to be perfectly known. Six synthetic CO_2 injection stages are considered to represent progressive plume migration (Figure 4). Under this assumption, passive-source FWI (Figure 5) consistently recovers the dominant ΔV_p anomaly at all stages, capturing both the spatial extent and migration direction of the plume.

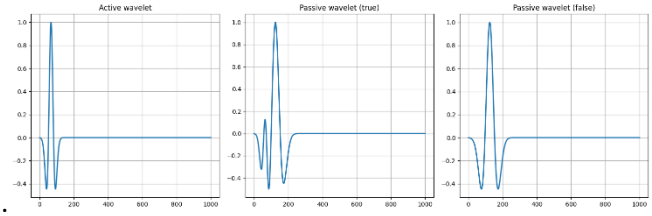


Figure 1. Source wavelets. From left to right: active-source wavelet; true passive source wavelet used for generating synthetic microseismic data; incorrect passive-source wavelet used in inversion.

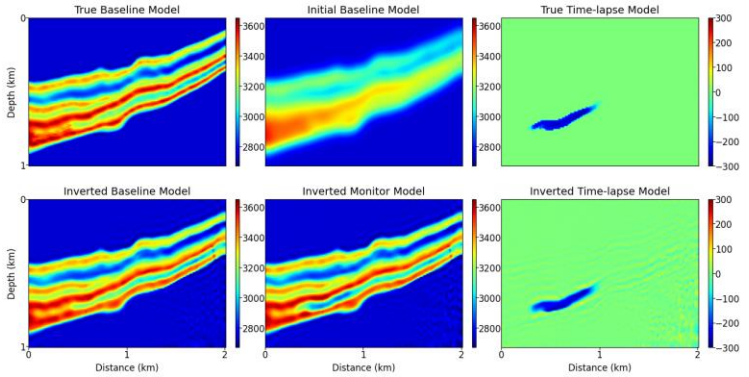


Figure 2. Active-source FWI results. Top row from left to right: true baseline velocity, true monitor velocity, and true time-lapse ΔV_p anomaly due to injected CO2. Bottom row from left to right: inverted baseline model, inverted monitor model, and inverted time-lapse anomaly.

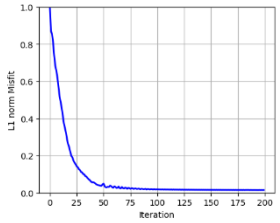


Figure 3. L1-norm misfit evolution for the active-source FWI of the monitor survey.

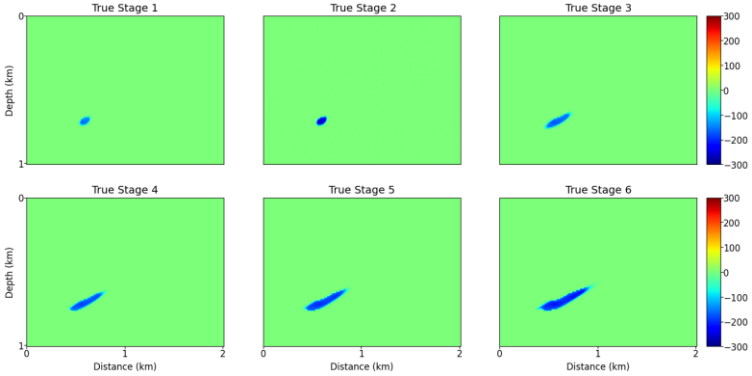


Figure 4. True time-lapse ΔV_p models for the six CO_2 migration stages.

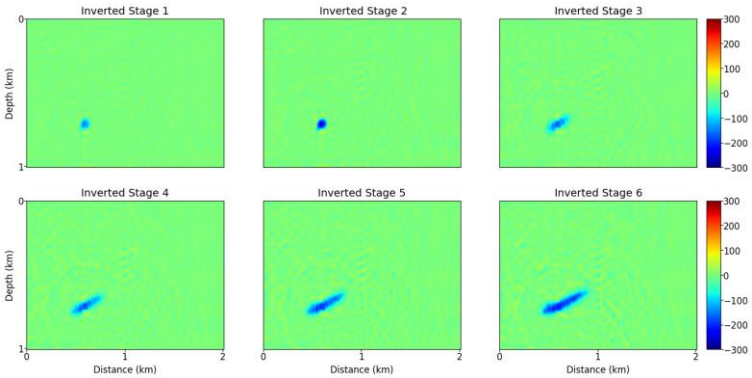


Figure 5. Passive-source FWI results using the true wavelet with two receiver wells: (1) one well 20 m left of the injector and (2) an additional well at x = 1000 m on the right side of the model.

To evaluate performance under more realistic conditions, passive-source FWI is repeated using an incorrect source wavelet (Figure 1), while the data are generated using the true wavelet. In this case, conventional passive waveform-based inversion fails (Figure 6). The recovered models are dominated by strong artifacts and cycle skipping, and the resulting ΔV_p distributions do not correspond to the true CO_2 plume geometry or its stage-to-stage evolution. These results demonstrate that, even when the underlying time-lapse signal is relatively strong, source mismatch alone can dominate the inversion and prevent reliable recovery of CO_2-induced velocity changes.

To mitigate source mismatch, three source-tolerant inversion strategies are applied to the same passive dataset. The envelope-based inversion (Figure 7) improves stability relative to conventional waveform misfits and recovers the general location of the CO_2-induced ΔV_p anomaly; however, the results remain spatially diffuse with poorly defined plume migration and boundaries. Choi's source-independent objectives (Figure 8) further reduce dependence on the unknown source wavelet and yield improved spatial localization with fewer coherent artifacts and migration trend, but the recovered plume still poorly defined plume boundaries. In contrast, the proposed method (Figure 9) produces the most stable and consistent results across all six injection stages, recovering the primary CO_2-related velocity anomaly with clear spatial localization, coherent stage-to-stage migration, and substantially reduced artifacts, indicating superior robustness to strong source mismatch.

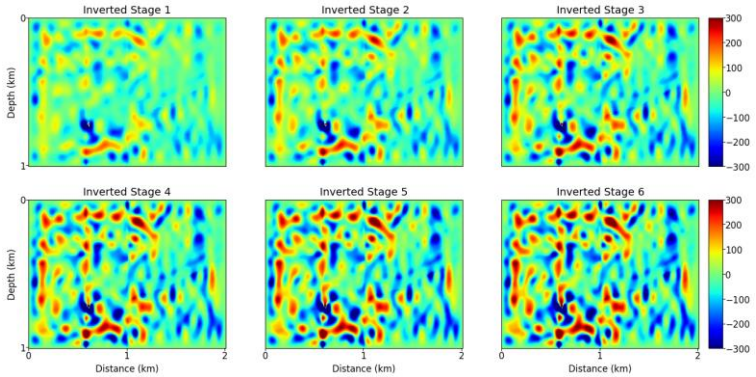


Figure 6. Passive-source FWI results when the inversion uses the incorrect wavelet while data are generated with the true wavelet. These artifacts reflect cycle skipping and phase inconsistency induced by the incorrect wavelet.

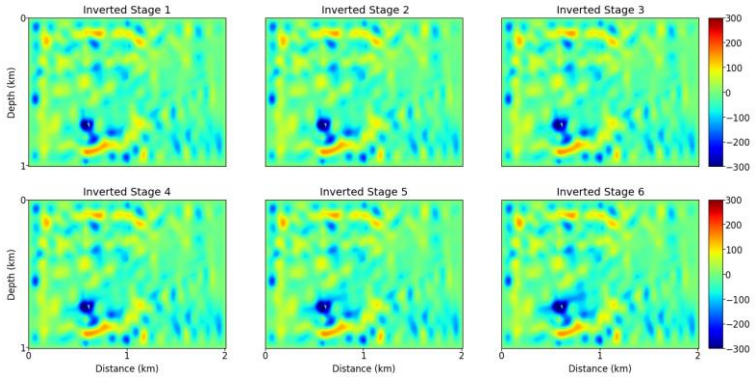


Figure 7. Passive-source FWI results using the envelope FWI.

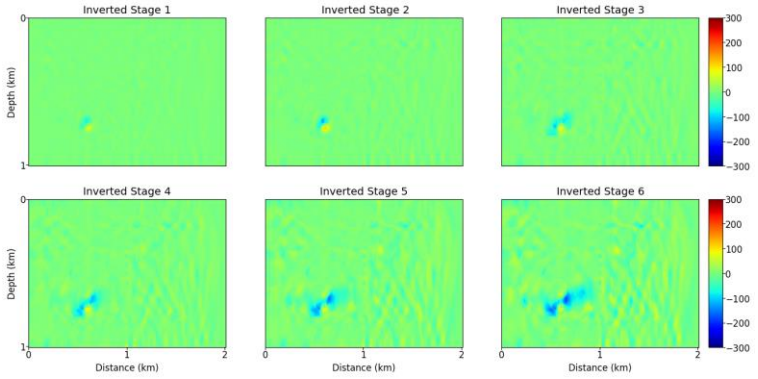


Figure 8. Passive-source FWI results using Choi's source-indepdent FWI.

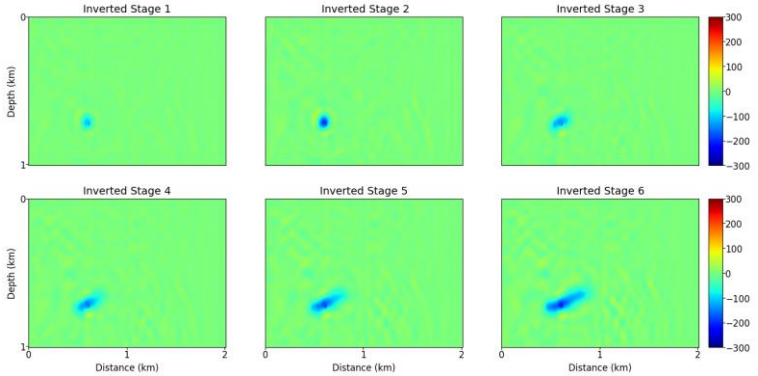


Figure 9. Passive-source FWI results using the proposed FWI method.

Conclusions

This study demonstrates that microseismic data can provide valuable time-lapse constraints for quasi-continuous CO_2 monitoring when integrated within a joint active–passive FWI framework. While active-source time-lapse FWI delivers reliable high-resolution imaging, its temporal sampling remains inherently sparse, and passive microseismic observations are strongly influenced by source uncertainty. Numerical results show that conventional passive-source FWI fails under realistic source mismatch conditions, whereas source-independent and source-tolerant formulations substantially improve inversion stability. Among the approaches examined, the proposed method achieves the most consistent recovery of CO_2-related velocity changes across multiple injection stages, successfully capturing plume geometry and migration trends despite significant wavelet mismatch. These findings indicate that robust passive FWI can effectively complement sparse active surveys and enable more frequent updates of subsurface CO_2 evolution, offering a practical pathway toward quasi-continuous seismic monitoring of geological CO_2 storage.

Acknowledgements

The sponsors of CREWES are acknowledged and thanked for continued support. This work was funded by CREWES industrial sponsors, and NSERC (Natural Science and Engineering Research Council of Canada) through the grants CRDPJ 543578-19 and ALLRP 606155-25. Further support of this work was provided by Emissions Reduction Alberta through the ACT4-SPARSE project.

References

Aragao, O., and Sava, P., 2020, Elastic full-waveform inversion with probabilistic petrophysical model constraints: Geophysics, 85, No. 2, R101–R111.

Asnaashari, A., Brossier, R., Garambois, S., Audebert, F., Thore, P., and Virieux, J., 2013, Regularized seismic full waveform inversion with prior model information: Geophysics, 78, No. 2, R25–R36.

Cai, X., Hu, Q., Innanen, K. A., Keating, S. D., Eaid, M. V., Macquet, M., and Lawton, D. C., 2025, Rapid repeat time-lapse vertical seismic profile imaging of co2 injection: Geophysics, 90, No. 2, B91–B99.

Cai X, Innanen K A, Eaid M V, et al. Multiazimuth elastic full-waveform inversion of fiber-optic and accelerometer vertical seismic profile data: A field example from the carbon management Canada Newell County Facility, Alberta, Canada[J]. Distributed Acoustic Sensing in Borehole Geophysics, 2024: 415-430.

Egorov, A., Pevzner, R., Bona, A., Glubokovskikh, S., Puzyrev, V., Tertyshnikov, K., and Gurevich, B., 2017, Time-lapse full waveform inversion of vertical seismic profile data: Workflow and application to the CO2CRC Otway project: Geophysical Research Letters, 44, No. 14, 7211–7218.

Hu, Q., Eaid, M. V., Innanen, K. A., Keating, S. D., and Cai, X., 2024, Estimation of rock physics properties via full waveform inversion of vertical seismic profile data recorded by accelerometer and fibre-optic sensors: Geophysical Journal International, 237, No. 2, 805–817.

Hu, Q., Grana, D., and Innanen, K. A., 2023, Feasibility of seismic time-lapse monitoring of CO2 with rock physics parametrized full waveform inversion: Geophysical Journal International, 233, No. 1, 402–419.

Huang, R., Zhang, Z., Wu, Z., Wei, Z., Mei, J., and Wang, P., 2021, Full-waveform inversion for ful lwavefield imaging: Decades in the making: The Leading Edge, 40, No. 5, 324–334.

Isaenkov, R., Pevzner, R., Glubokovskikh, S., Yavuz, S., Shashkin, P., Yurikov, A., Tertyshnikov, K., Gurevich,B., Correa, J., Wood, T. et al., 2022, Advanced time-lapse processing of continuous das vsp data for plume evolution monitoring: Stage 3 of the co2crc otway project case study: International Journal of Greenhouse Gas Control, 119, 103,716.

O'Brien, J., Kilbride, F., and Lim, F., 2004, Time-lapse vsp reservoir monitoring: The Leading Edge, 23, No. 11, 1178–1184.

Pan, W., Innanen, K. A., and Wang, Y., 2020, Parameterization analysis and field validation of VTI-elasticfull-waveform inversion in a walk-away vertical seismic profile configuration: Geophysics, 85, No. 3, B87–B107.

Prieux, V., Brossier, R., Operto, S., and Virieux, J., 2013, Multiparameter full waveform inversion of multicomponent ocean-bottom-cable data from the valhall field. part 1: Imaging compressional wave speed, density and attenuation: Geophysical Journal International, 194, No. 3, 1640–1664.

Vigh, D., Cheng, X., Xu, J., and Jiao, K., 2023, Forge ahead in acquisition and model building via fullwaveform inversion: Gulf of Mexico case study: Geophysics, 88, No. 5, B285–B295.

Virieux, J., and Operto, S., 2009, An overview of full-waveform inversion in exploration geophysics: Geophysics, 74, No. 6, WCC1–WCC26.

Zhang, T., Cai, X., Hall, K., and Innanen, K., 2025, Assessing the value of combined use of distributed acoustic sensing and multicomponent vertical seismic profiling data with network-based full-waveform inversion and uncertainty quantification: A case study in alberta, canada: Geophysics, 90, No. 1, B29–B47.